Available online at www.sciencedirect.com

SCIENCE DIRECT®

Polymer Degradation and Stability 87 (2005) 535–542

Polymer Degradation and Stability

www.elsevier.com/locate/polydegstab

Polylactide/montmorillonite nanocomposites: study of the hydrolytic degradation

M.-A. Paul[a], C. Delcourt[a], M. Alexandre[a], Ph. Degée[a], F. Monteverde[b], Ph. Dubois[a,*]

[a] *Laboratory of Polymeric and Composite Materials (LPCM), University of Mons-Hainaut, 20 place du Parc, 7000 Mons, Belgium*
[b] *Laboratory of Analytic and Inorganic Chemistry (LAIC), University of Mons-Hainaut, 20 place du Parc, 7000 Mons, Belgium*

Received 13 June 2004; accepted 23 October 2004
Available online 8 December 2004

Abstract

Hydrolytic degradation of polymer layered silicate nanocomposites based on polylactide matrix (PLA) and (organo-modified) montmorillonites was investigated in phosphate buffer solution for more than five months. While natural unmodified montmorillonite-Na^+ led to the formation of a microcomposite, mainly intercalated nanocomposites were prepared by melt blending PLA with 3 wt% of montmorillonite organo-modified either by 2-ethylhexyl (hydrogenated tallowalkyl) ammonium cations (Cloisite®25A) or by bis-(2-hydroxyethyl) methyl tallowalkyl ammonium cations (Cloisite®30B). The evolution of molecular weight of the matrix as well as its crystallinity with the hydrolysis time has been recorded by size exclusion chromatography (SEC) and differential scanning calorimetry (DSC), respectively. Thermogravimetric analyses (TGA) performed on the microcomposite based on Cloisite®Na^+ has shown that the thermal stability of the materials decreased proportionally to the decreasing PLA molecular weight along the hydrolysis time. Moreover, in parallel to the morphology of the composites, the relative hydrophilicity of the clay layers has been shown to play a key role in the hydrolytic degradation of the PLA chains.

Keywords: Polylactide; Nanocomposite; Montmorillonite; Clay; Degradation; Hydrolysis

1. Introduction

The biodegradation of synthetic polymers is a complex process, which can proceed via hydrolysis (most often catalysed by enzymes) and/or oxidation (UV- or thermo-induced). The stereoconfiguration and possible crystallinity, relative hydrophobicity of the polymer matrix, presence of substituents, or even filler and conformational flexibility contribute to the biodegradability of synthetic polymers with hydrolysable and/or oxidisable linkages in their main chain. On the other hand, the morphology of the polymer samples or the material structure as recovered after loading with a given filler, greatly affect their rate of biodegradation.

Aliphatic polyesters, and particularly polylactide (PLA), are currently deserving a particular attention in the area of environmentally degradable polymer materials. They are well suited for the preparation of disposable devices because of their biodegradability. Indeed, one of the main characteristics of PLA matrix, which is currently responsible for many of its applications, stands in its easiness to degrade by enzymatic [1] or hydrolytic way [2,5].

The hydrolytic degradation of PLA is a well-known process. It happens mainly in the bulk of the material and not from its surface [3]. The hydrolytic chains cleavage proceeds preferentially in amorphous regions, leading therefore to an increase of the polymer global crystallinity [4]. This explains the much faster hydrolysis

---

* Corresponding author. Tel.: +32 65 37 34 80; fax : +32 65 37 34 84.

E-mail address: philippe.dubois@umh.ac.be (Ph. Dubois).

0141-3910/$ - see front matter © 2004 Elsevier Ltd. All rights reserved.
doi:10.1016/j.polymdegradstab.2004.10.011

rate of the amorphous P(D,L-LA) compared to semi-crystalline P(L,L-LA). The formation of lactic acid oligomers which directly follows from this chain scission, increases the carboxylic acid end groups concentration in the medium. These carboxylic functions are known to catalyse the degradation reaction. In conclusion, the hydrolytic degradation of PLA is a self-catalysed and self-maintaining process [5]. Such mechanisms can be affected by various factors, such as chemical structure, molar mass and its distribution, purity, morphology, shape and history of the specimen, as well as the conditions under which the hydrolysis is conducted [6,7].

In this context, even if nanocomposites based on aluminosilicate layers and biodegradable polymer matrices have already been extensively studied in terms of mechanical, thermal, fire retardancy or crystallisation behaviours [8], biodegradation and more specially hydrolysis still need to be investigated in order to characterise the influence of the filler on such a process. Clearly PLA layered silicate nanocomposites display much improved properties as compared to the unfilled PLA and corresponding microcomposites. However, a key-question that remains to be addressed concerns the possible influence of the organo-clay filler on the polyester matrix biodegradation.

Recently, Sinha Ray et al. have studied the degradation of PLA/organo-clay nanocomposites by composting at 58 °C. These nanocomposites were prepared by melt blending the polyester with a montmorillonite organo-modified by trimethyl octadecyl ammonium cations [9,10]. They reached to the conclusion that the (bio)degradation of the nanocomposites operates more rapidly than the unfilled PLA actually, in opposition to the behaviour that could be expected. Indeed, while considering the nanoclay platelets as totally impermeable species, the penetration of diverse permeants, such as oxygen or water, should be delayed, such phenomenon being directly responsible for the improvement of nanocomposite barrier properties in respect of the matrix [8]. After two months in compost a PLA-based nanocomposite filled with 4 wt% of such an organo-modified montmorillonite was completely degraded, while the unfilled PLA sample was recovered in the form of very small pieces.

Therefore it was of interest to check whether montmorillonite, organo-modified or not, behaves in a similar way on the hydrolytic degradation of the PLA matrix.

In this paper, we therefore aim at reporting about the carefully controlled hydrolytic degradation behaviour of nanocomposites based on polylactide and three different types of (organo-modified) montmorillonites. A degradation study in buffer phosphate medium (0.1 M, pH fixed at 7.4) at 37 °C, has been carried out on composites prepared by melt blending PLA with 3 wt% of Cloisite®Na$^+$, Cloisite®25A and Cloisite®30B, respectively (see Section 2). The unfilled PLA matrix has been also studied as a reference.

2. Experimental

2.1. Materials

Poly(D,L-lactide) with 30% of D-lactoyl unity (PLA) was obtained from Cargill-Dow S.A. ($M_n = 85,000$, $M_w/M_n = 1.9$) and used as the polyester matrix. Three different clays were employed and supplied by Southern Clay Products. The unmodified montmorillonite-Na$^+$ (Cloisite®Na$^+$) has a cation exchange capacity of 92 meq/100 g. The other two clays were organo-modified montmorillonites. Cloisite®25A is modified by dimethyl-2-ethylhexyl (hydrogenated tallowalkyl) ammonium cations and Cloisite®30B with bis-(2-hydroxyethyl) methyl tallowalkyl ammonium cations. The level of organic materials contained in the organo-modified clays was determined by thermogravimetric analyses (TGA) (Table 1).

2.2. Samples preparation

Before processing, PLA was dried overnight at 60 °C under reduced pressure and stored under vacuum in the presence of humidity absorbent. The (organo-)clays were also dried at 40 °C under reduced pressure for 4 h. Blending of PLA with clay particles (3 wt% in inorganic content, independently of the amount of organic modifier) was conducted in presence of 0.3 wt% of Ultranox®626 stabilizer on a Brabender counter-rotating

Table 1
Composite description

Composite code	Clay			Interlayer distance (Å)	
	Type	Ammonium cations	Organic content (wt%)	In clay	In composite
M3Na	Cloisite®Na$^+$	–	–	12.1	–[a]
N3A25	Cloisite®25A	$(C_{18}H_{37})\text{-}N^+[CH_2\text{-}CH(C_2H_5)\text{-}C_3H_8](CH_3)_2$	26.9	20.4	31.4
N3B30	Cloisite®30B	$(C_{18}H_{35})\text{-}N^+(C_2H_4OH)_2CH_3$	20.1	18.4	36.4

[a] No diffraction peak detected.

mixer with a rotation speed of 20 rpm for 4 min, then at 60 rpm for 3 min. The processing temperature was set at 180 °C. Three-millimeter thick plates were then shaped by compression moulding at 180 °C. The material was pressed under 150 bars for 120 s, followed by a cycle where the pressure was kept successively at 20, 80, 140 bars for 5 s and then released for 1 s after each pressure moulding increase (in order to get rid of any bubbles), and finally under 30 bars for 240 s. The samples were then cooled down by compressing at 15 °C under 150 bars for 5 min.

2.3. Hydrolysis tests

Practically, before starting the hydrolysis tests, the samples were shaped as films of about 0.5 mm in thickness following the same program reported in the 3 mm thick plate sample preparation. In a second step, each film was cut into $1.3 \times 3.0\ \mathrm{cm}^2$ rectangular specimen (three specimens per sample). Each specimen was then dipped in a flask containing 25 ml of 0.1 M phosphate buffer at pH 7.4. The flasks were immersed in a water bath at 37 °C. At predetermined periods (one week, two weeks, one month, two and a half months, and five and a half months) the specimen were picked out of the buffered solution and rinsed several times with distilled water. Finally, the residual water was wiped off from the sample surface before drying by wrapping it in a small paper bag placed in a desiccator.

2.4. Characterisation

Thermogravimetric analyses were performed using a Hi-Res TGA 2950 thermogravimetric analyzer from TA instruments with a heating ramp of 20 K/min under air flow (74 cm^3/min) from room temperature to 600 °C.

The thermal behaviour was measured with a DSC 2920 from TA instruments, with a heating and cooling ramp of 10 K/min from −50 °C to 200 °C under nitrogen flow and the values were recorded during the first heating scan. The morphological analysis by X-ray diffraction was performed on a Siemens D5000 diffractometer using Cu(K_α) radiation (wavelength: 1.5406 Å) at room temperature in the range of $2\theta = 1.5$ to 30° with a scanning rate of 2°/min. Molecular weight determination of PLA was carried out after eliminating the clay by filtration of samples dissolved in chloroform. The catalyst residues were removed by liquid–liquid extraction with a 0.1 M HCl aqueous solution and PLA was recovered by precipitation from cold methanol. Size exclusion chromatography measurements were performed in THF (with 2 v/v % of triethylamine added) at 35 °C using a Polymer Laboratory (PL) liquid chromatograph equipped with a PL-DG802 degasser, an isocratic HPLC pump LC1120 (flow rate: 1 ml/min), a Basic-Marathon autosampler, a PL-RI refractive index detector and four columns: a guard column PLgel 10 μm (50 × 7.5 mm) and three columns PLgel 10 μm mixed-B (300 × 7.5 mm). Molecular weights and molecular distributions were calculated by reference to a universal calibration curve relative to PS standard, and using the Kuhn–Mark–Houwink equation for PLA in THF: $M_\mathrm{n}(\mathrm{PLA}) = 0.4055 \times M_\mathrm{n}(\mathrm{PS})^{1.0486}$ [11].

3. Results and discussion

Before starting the hydrolysis experiments, the morphology of each composite was determined using wide-angle X-ray scattering. As a result of PLA melt blending with 3 wt% of (organo-modified) montmorillonite, a microcomposite was recovered when Cloisite®Na$^+$ was concerned, while intercalated nanocomposites were prepared starting from Cloisite®25A or Cloisite®30B (Table 1). These observations are in perfect agreement with the previously published data [12]. Actually it is worth recalling that the absence in the XRD pattern of the diffraction peak corresponding to the sodium montmorillonite has been attributed to the tiny content in unmodified clay (3 wt%) dispersed in the PLA matrix. Indeed, already for Cloisite®Na$^+$ alone, the XRD pattern displayed a weak peak around 7.5°, i.e., corresponding to a basal spacing of 12.1 Å.

The changes in the general aspect of the sample upon hydrolysis could be first of all visually judged. As revealed in Fig. 1, a significant change in the sample opacity could be noticed, already after one week of immersion in buffered solution. Although the most pronounced change was observed for Cloisite®-Na$^+$-based blend (i.e., the microcomposite) both nanocomposites filled with 3 wt% of organo-clay (Cloisite®25A or Cloisite®30B), as well as the unfilled PLA matrix, underwent some modifications in their macroscopic aspect. Increasing the hydrolysis time led to an increase in relative opacity of the materials. In addition, while the other samples kept a relatively planar geometry, the microcomposite specimen started to curve after one month of hydrolysis (Fig. 1, see arrow).

After two and a half months in buffered solution, the curvature of the microcomposite specimen again increased, as evidenced by the transverse observation displayed in Fig. 2. It must be noted that the Cloisite®30B-based nanocomposite specimen had its extremities slightly curving up as well (Fig. 2, see arrow). Finally, after five and a half months of hydrolytic degradation, all the composites, both micro- and nanocomposites, turned white and became extremely brittle. More particularly, the microcomposite was recovered in small pieces after the drying step which directly followed the sample removal from phosphate buffer (Fig. 3).

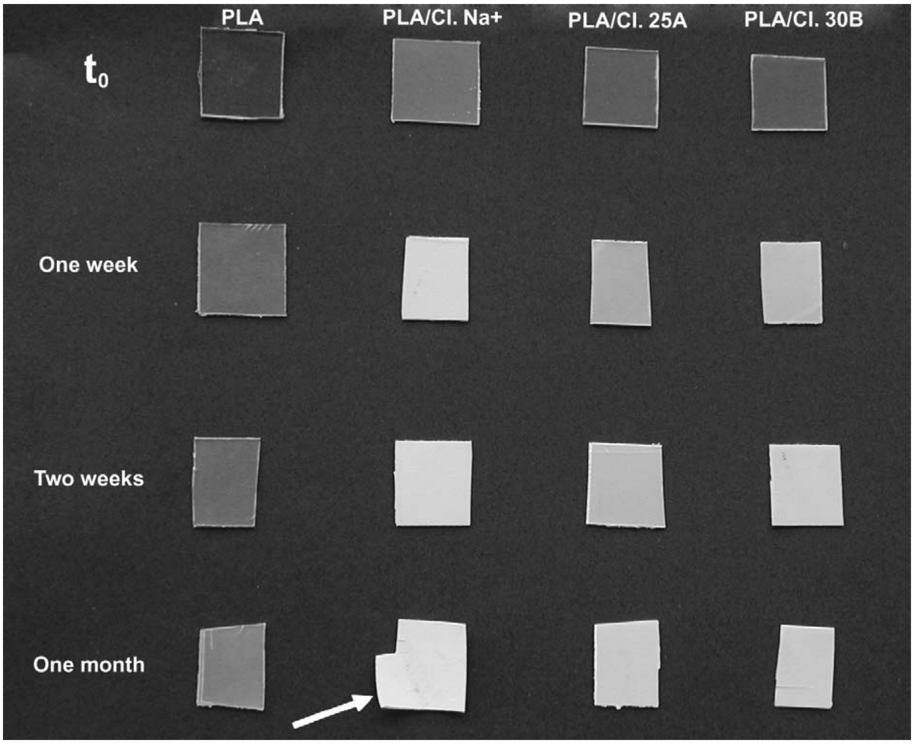

Fig. 1. Changes in sample visual aspect upon one month of hydrolysis for the PLA matrix, the microcomposite based on 3 wt% of Cloisite®Na$^+$ (PLA/Cl.Na), and the intercalated nanocomposites based on 3 wt% of Cloisite®25A (PLA/Cl.25A) and Cloisite®30B (PLA/Cl.30B), respectively.

The modification of the opacity of each sample can be explained by various phenomena occurring all along the degradation. Indeed, the changes in appearance are directly related to the light diffusion through the material. Such diffusion can be altered either by the formation of holes in the bulk of the specimen during the degradation or by an evolution in crystallinity of the polymer matrix. Since the hydrolytic degradation of the polyester chains is known to take place in the amorphous phase of the matrix [4], this phenomenon is expected to increase the PLA crystallinity, which is translated by an increase in the overall opacity of the samples.

In order to shed some light on the impact of the hydrolysis degradation on the composite properties, the alteration of the molecular weight of PLA chains extracted from the different samples was analysed after their recovery from the buffered solution (see Section 2). In parallel, DSC analyses carried out on as-recovered, slightly dried samples, have shown the influence of degradation time on thermal transitions (T_g, T_c and T_m) as well as on crystallisation (ΔH_c) and melting (ΔH_m) enthalpies. For the sake of clarity, the influence of time on the all aforementioned parameters are discussed in Figs. 4–7. It must be noted that each data given in these figures represents the average value calculated from the results obtained for three individual samples of each composition.

Fig. 4 presents the changes in PLA molecular weight as a function of hydrolysis time. Concerning both unfilled polyester matrix and the intercalated nanocomposite based on 3 wt% Cloisite®25A, the first month of hydrolysis can be considered as an induction period, along which M_n is relatively constant around 60,000 and 66,000, respectively. After five and a half months, the molecular weight of the unfilled PLA sample decreased by 41.6% with respect to its initial value. In parallel, the losses in M_n for intercalated

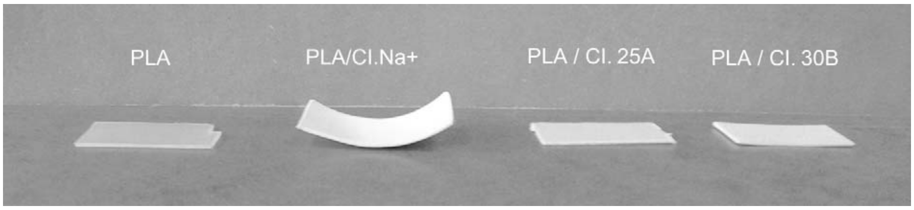

Fig. 2. Transverse view of both unfilled PLA and composites after two and a half months of hydrolysis (Cl. stands for Cloisite®).

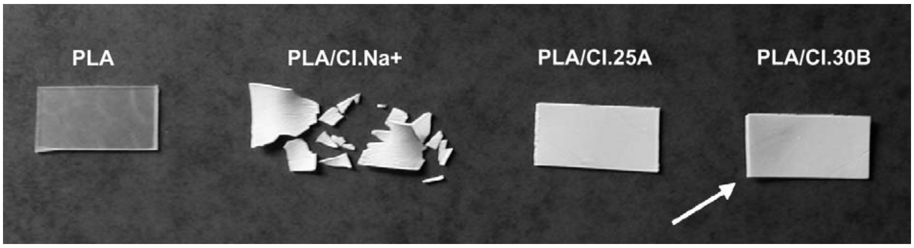

Fig. 3. Visual aspect of PLA matrix, microcomposite based on Cloisite®Na$^+$ and nanocomposites based on Cloisite®25A and 30B, respectively, after five and a half months of hydrolysis (Cl. stands for Cloisite®).

nanocomposites based on Cloisite®25A and Cloisite®30B were 71.2% and 79.2%, respectively. However, it must be noted that the degradation recorded for Cloisite®30B-based nanocomposite was extremely regular, as denoted by the linear regression of the M_n evolution vs. hydrolysis time. Finally, the most significant degradation in terms of molecular weight decrease is assigned to the microcomposite, i.e. Cloisite®Na$^+$-based blend. Indeed, the degradation appears much faster compared to the other samples: at the end of the hydrolysis study, the PLA chains extracted from this microcomposite specimen have lost 93.1% of their initial length.

Moreover, it must be noted that neither the unfilled PLA nor the nano- or microcomposites have lost weight upon hydrolysis. Such behaviour is not really surprising as the species formed by hydrolysis, i.e., shorter PLA chains and cyclic oligomers are not soluble in the buffer solution. Only dimer or trimer of lactic acid as well as lactic acid itself solubilize in phosphate buffered medium.

Focusing attention on thermal transitions and crystallisation behaviour of the polyester matrix, it can be firstly noted that the polyester T_g, in unfilled PLA, is relatively constant and stands near 62 °C even after more than five months of hydrolysis (Fig. 5). In sharp contrast, as far as the microcomposite is concerned, PLA matrix T_g drops by approximately 10 °C only after one month in buffer (while it has not been significantly modified for the other samples). For Cloisite®30B-based nanocomposite, T_g starts to decrease after one month of hydrolysis, while, more than two and a half months are necessary to significantly decrease the T_g of the PLA matrix filled with Cloisite®25A. Such a decrease in T_g for polyester matrix can be explained by both the reduction of the PLA molecular weight and by the known plasticising effect of lactic acid oligomers formed upon degradation reaction.

As evidenced in Fig. 6(a), the crystallisation enthalpy (ΔH_c) has already increased after one week of hydrolysis for both micro- and nanocomposites. In contrast, an induction period of approximately one month is necessary to see the crystallisation enthalpy of the unfilled PLA matrix increasing to reach the same definitive level as nanocomposites, located at ca. 30 J/g$_{PLA}$ after five and a half months. The rapid growth of ΔH_c in the PLA-based composites could be explained by

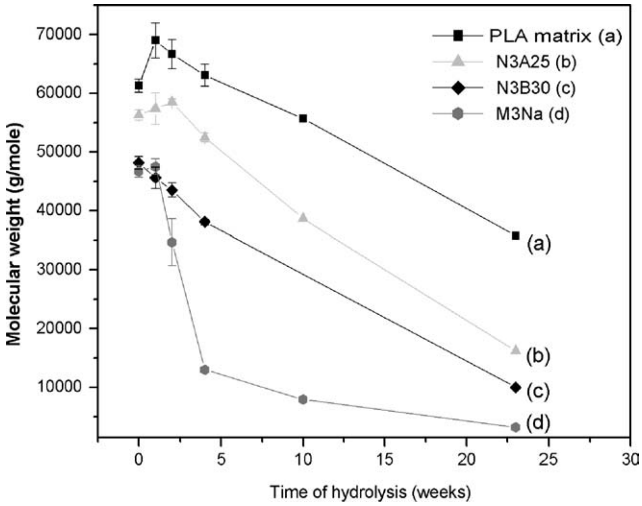

Fig. 4. M_n evolution vs. hydrolysis time of PLA matrix (curve (a)) and PLA composites filled with either 3 wt% of Cloisite®25A (N3A25, curve (b)), Cloisite®30B (N3B30, curve (c)) or 3 wt% of Cloisite®Na$^+$ (M3Na, curve (d)).

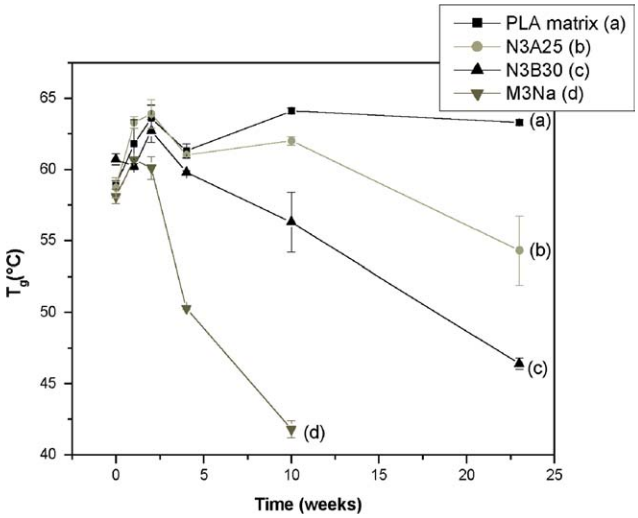

Fig. 5. Evolution of T_g vs. hydrolysis time for unfilled PLA matrix (curve (a)) and PLA composites filled with 3 wt% Cloisite®25A (curve (b)), Cloisite®30B (curve (c)) or Cloisite®Na$^+$ (curve (d)).

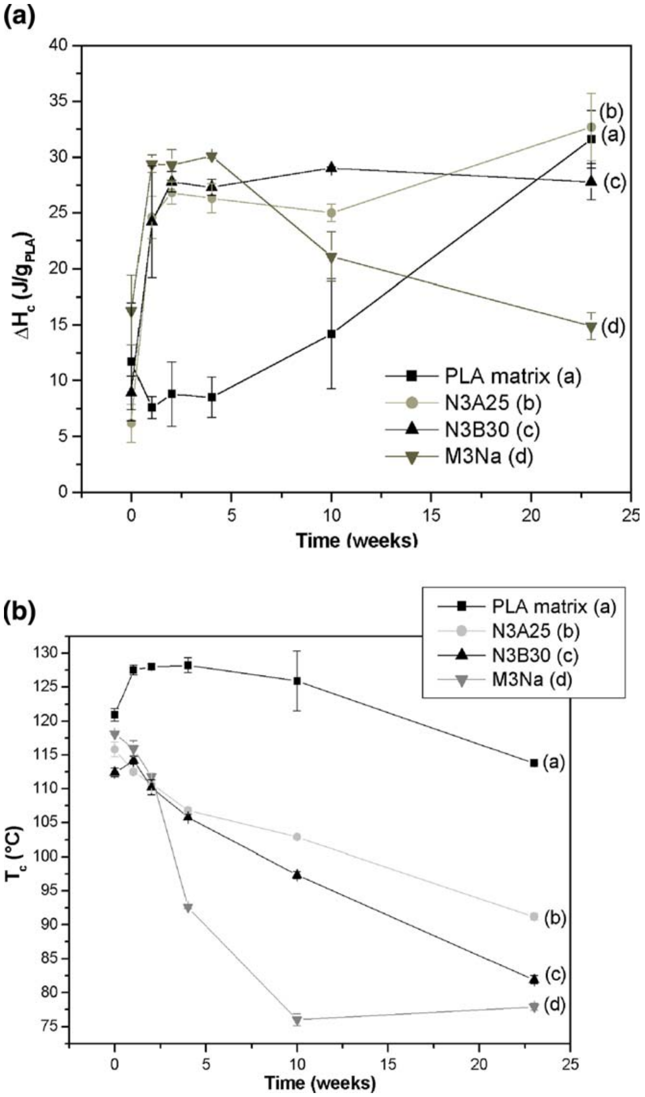

Fig. 6(a) and (b). Evolution of ΔH_c (Fig. 6(a)) and T_c (Fig. 6(b)) vs. hydrolysis time for PLA matrix (curves (a)), the microcomposite based on 3 wt% of Cloisite®Na$^+$ (curves (d)) and the nanocomposites based on 3 wt% Cloisite®25A (curves (b)) and Cloisite®30B (curves (c)), respectively.

the nucleating ability of the aluminosilicate filler. Although ΔH_c is quite similar for each composite after one month of hydrolysis, the higher values are recorded for Cloisite®Na$^+$-based blend. Moreover, while a plateau is finally reached for nanocomposites at longer degradation time, ΔH_c of PLA matrix involved in the microcomposite starts to decrease in agreement with the aforementioned large reduction in molecular weight compared to other samples.

The microcomposite clearly undergoes faster and more significant degradation than the other materials. Such behaviour can be explained by the relatively high hydrophilicity of Cloisite®Na$^+$ compared to Cloisite®30B (or even more to Cloisite®25A). This hydrophilicity allows the water molecules to penetrate more easily within the material to trigger the hydrolytic degradation process. A second key parameter to take into account for explaining such a fast degradation is the specific morphology of the microcomposite based on Cloisite®-Na$^+$. In such a structure, the clay platelets are stacked in micrometer-size particles, the diffusion pathway of the water molecules is made easier and faster than in intercalated Cloisite®25-based nanocomposite and Cloisite®30B-based blend in which the aluminosilicate layers are much more homogeneously distributed throughout the PLA matrix.

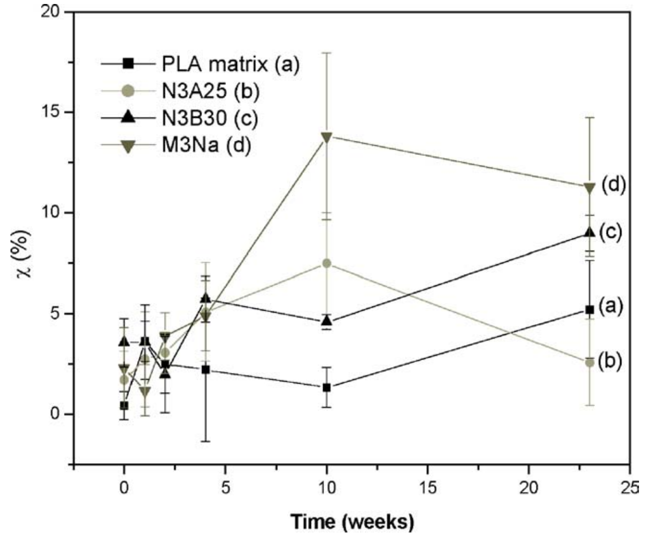

Fig. 7. Evolution of the crystallinity of PLA chains vs. hydrolysis time for unfilled PLA matrix (curve (a)), the nanocomposites based on 3 wt% of either Cloisite®25A (curve (b)), or Cloisite®30B (curve (c)) and a microcomposite based on 3 wt% of Cloisite®Na$^+$ (curve (d)).

As far as the evolution of T_c(PLA) is concerned (Fig. 6(b)), it can readily be related to the evolution of the molecular weight since it is well known that shorter PLA chains tend to crystallise at lower temperature.

The evolution of the global crystallinity (χ) of the PLA chains during hydrolysis (Fig. 7) can be deduced through the evolution of both ΔH_c and ΔH_m. Initially, χ is very weak (between 1 and 4%), indicating a quasi amorphous structure. In buffer phosphate medium, χ remains relatively constant for the first two weeks whatever the samples considered. After one month, χ of PLA matrix in both micro- and nanocomposites increases to reach a maximal value after two and a half months in the buffer solution. Since none of the samples have experienced weight loss upon hydrolysis, such an increase in crystallinity cannot be ascribed to a decrease of the relative content in amorphous phase. This increase has to be attributed to an effective crystallisation occurring during hydrolysis. One possible mechanism that would allow for such crystallisation would imply both the decrease in the PLA molecular weight and a plasticisation of PLA by water and buffer

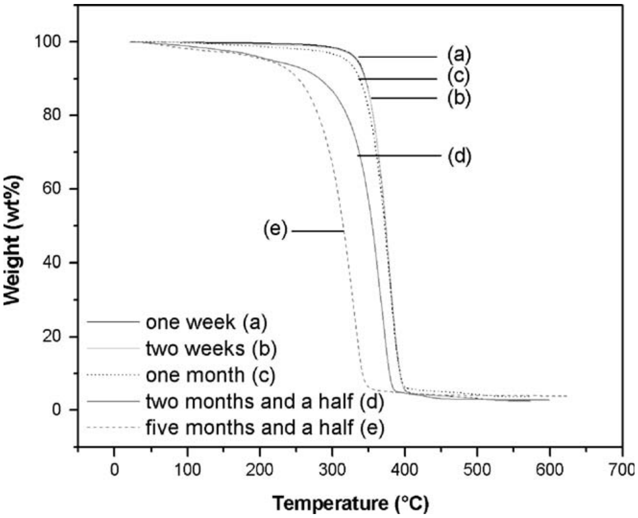

Fig. 8. Thermogravimetric analyses of Cloisite®Na$^+$-based microcomposite after one week (curve (a)), two weeks (curve (b)), one month (curve (c)), two and a half months (curve (d)) and five and a half months (curve (e)).

molecules as well as by lactic acid oligomers that would give sufficient mobility to the polymer chains to organise and crystallise further.

Such a mechanism would explain why the unfilled PLA matrix has kept the same relative total crystallinity even after five and a half months of hydrolysis, while the maximal increase in χ has been observed for Cloisite®Na$^+$-based microcomposite. At the end of the considered degradation time, thus after five and a half months, Cloisite®Na$^+$-based microcomposite displays a higher crystallinity, followed by Cloisite®30-based nanocomposite and the unfilled PLA matrix. The lower χ value evidenced for Cloisite®25A could be explained by the fact that Cloisite®25A proved very efficient to limit the diffusion of water molecules throughout the matrix.

In terms of thermal stability, no influence of hydrolysis time on the maximum degradation temperature has been detected by TGA analysis for the nanocomposite based on Cloisite®25A, even if the PLA M_n has decreased from 56,300 to 16,200 at the end of the study. Indeed the temperature of maximum degradation was around 385 °C whatever the hydrolysis time. It seems therefore that in case of Cloisite®25A the lost in thermal stability due to M_n reduction is counterbalanced by the stabilising effect provided by the nanoclay intercalation. Such an effect is indirectly confirmed by the changes in thermogram curves recorded for the unfilled PLA matrix, for which a shift of the thermograms towards lower temperature appears after two and a half months of degradation (corresponding to an M_n drop of 9.1%) compared to the initial value. In case of Cloisite®30B-based nanocomposite such a shift in the thermogram curve is only remarkable after five and a half months of hydrolysis. Finally, thermogravimetric analyses have shown a regular change of the maximum degradation temperature of the polyester matrix filled with Cloisite®Na$^+$ towards lower temperature with the hydrolysis time, as expected from the molecular weight decrease (Fig. 8).

In order to analyse the morphological evolution in the bulk of both unfilled PLA matrix and PLA-based composites during the hydrolysis process, scanning electron microscopy analyses (SEM) have been performed on samples before hydrolysis as after two and a half months and five and a half months of degradation, respectively.

After more than five months in buffered solution, neither the unfilled polyester matrix nor the Cloisite®25A-based nanocomposite had undergone structural modification. In contrast, when considering the microcomposite prepared with Cloisite®Na$^+$, the degradation of the matrix already taking place after two months of hydrolysis is shown by the appearance of holes homogeneously distributed in the entire material (Fig. 9(a) and (b)).

After five and a half months of degradation, the holes seem to coexist with elongated cracks (Fig. 10, surrounded area). Concerning the nanocomposite based on Cloisite®30B, a significant change in the overall morphology can be observed only at the end of the

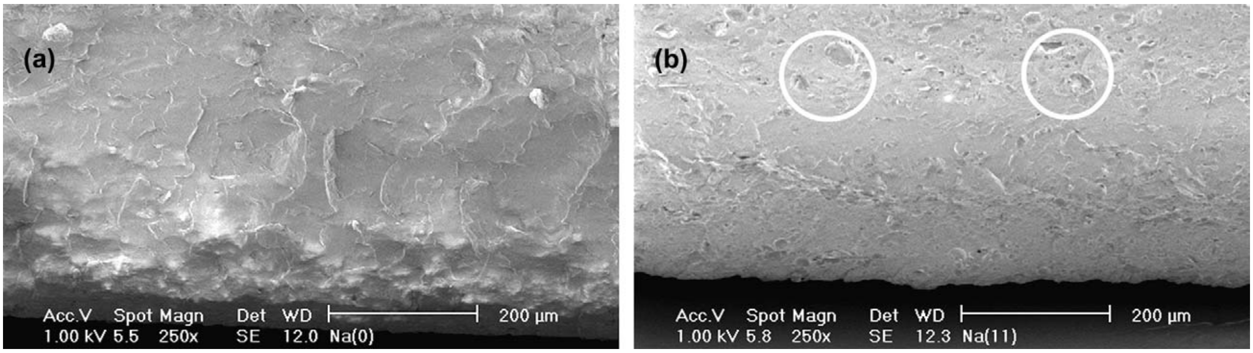

Fig 9. SEM pictures showing a cryofracture surface of the Cloisite®Na$^+$-based microcomposite before hydrolysis (a) and after two and a half months of hydrolysis (b); holes are highlighted by white circles ($G = 250\times$).

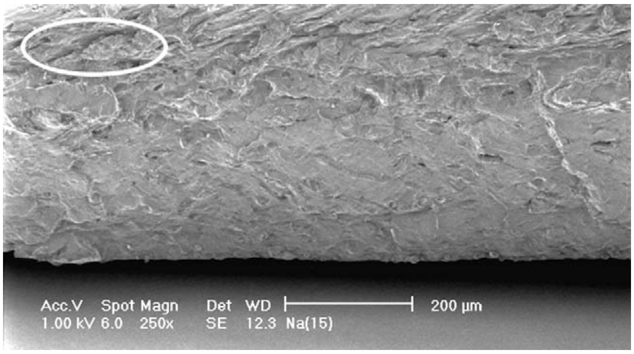

Fig. 10. SEM picture recorded for a cryofracture surface of the Cloisite®Na$^+$-based microcomposite after five and a half months of hydrolysis; surrounded area highlights a typical elongated crack ($G = 250\times$).

degradation study. Similarly to Cloisite®Na$^+$-filled microcomposites, the intercalated nanocomposite matrix is pitted with small holes (Fig. 11).

Clearly, the hydrolytic degradation of PLA matrix again operates in the bulk of the material, even if the polyester matrix is filled with micro- or nanofillers. Moreover, it has been highlighted that the degradation is directly related to the relative hydrophilicity of the filler. Indeed, the composites, which have undergone the maximum degradation, are those prepared with Cloisite®Na$^+$.

4. Conclusions

In order to understand to which extent the incorporation of montmorillonite, organo-modified or not, influences the degradation behaviour of the PLA matrix, hydrolytic degradation of composites based on the same amount (3 wt%) of Cloisite®Na$^+$, Cloisite®25A and Cloisite®30B has been investigated for more than five months, and directly compared to the unfilled polyester. As a result, it seems that the faster hydrolysis, leading to an increase of the crystallinity of the PLA matrix, is found for the Cloisite®Na$^+$-based blend, i.e., to the microcomposite structure. It has also been concluded that both composite structures, either microcomposite or intercalated nanocomposite, and the relative hydrophilicity of the clay play determining roles in the hydrolytic degradation process. Indeed, the more hydrophilic the filler, the more pronounced is the degradation.

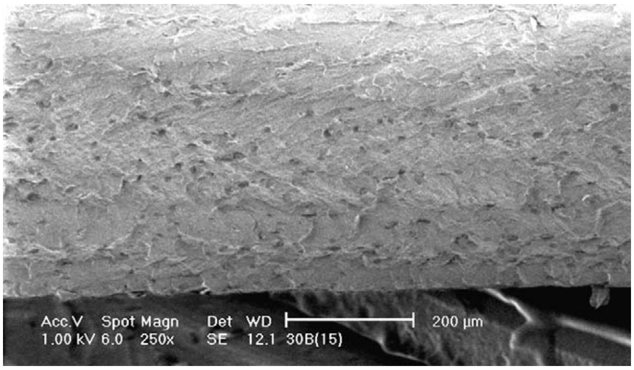

Fig. 11. SEM picture showing a cryofracture surface of the Cloisite®30B-based nanocomposite after five and a half months of hydrolysis ($G = 250\times$).

Acknowledgments

M.-A. Paul thanks the F.R.I.A. (Fonds pour la Recherche Industrielle et Agricole) for her PhD grant. Authors are very grateful for the financial support from "Région Wallonne" and European Community (FEDER, FSE) in the frame of "Pôle d'Excellence Materia Nova". LMPC thanks the Belgian Federal Government Office of Science Policy (STC-PAI 5/3). C. Delcourt is much indebted to the "Région Wallonne Programme WDU-TECMAVER". Prof. André Rulmont is greatly thanked for his help in the X-ray diffraction analyses.

References

[1] Edlund U, Albertsson A-C. Degradable polymer microspheres for controlled drug delivery. Adv Polym Sci 2001;157:67–112.
[2] Scott G. Degradable polymers: principles and applications. 2nd ed. 2002.
[3] Grizzi I, Garreau H, Li S, Vert M. Hydrolytic degradation of devices based on poly(DL-lactic acid) size-dependence. Biomaterials 1995;16:305–11.
[4] Hakkarainen M. Aliphatic polyesters: abiotic and biotic degradation and degradation products. Adv Polym Sci 2001;157:113–38.
[5] Tsuji H, Ikada Y. Properties and morphology of poly(L-lactide). 4. Effects of structural parameters on long-term hydrolysis of poly(L-lactide) in phosphate-buffered solution. Polym Degrad Stab 2000;67:179–89.
[6] Li S, Vert M. Biodegradation of aliphatic polyesters. In: Scott G, Gilead D editors. Degradable polymers: principles and applications. London: Chapman & Hall; 1995, p. 43–87.
[7] Vert M, Schwach G, Coudane J. Present and future of PLA polymer. J Mater Sci – Pure Appl Chem 1995;A32(4):787–96.
[8] Alexandre M, Dubois Ph. Mater Sci Eng 2000;R28(1–2):1–63.
[9] Sinha Ray S, Yamada K, Okamoto M, Ueda K. Polylactide-layered silicate nanocomposite: a novel biodegradable material. Nano Lett 2002;2(10):1093–6.
[10] Sinha Ray S, Yamada K, Okamoto M, Ueda K. New polylactide-layered silicate nanocomposites. 2. Concurrent improvements of material properties, biodegradability and melt rheology. Polymer 2003;44:857–66.
[11] Degée Ph, Dubois Ph, Jérôme R. Bulk polymerization of lactides initiated by aluminum isopropoxide. 3. Thermal stability and viscoelastic properties. Macromol Chem Phys 1997;198:1985–95.
[12] Pluta M, Galeski A, Alexandre M, Paul M-A, Dubois Ph. Poly(lactide)/montmorillonite nano- and micro-composites prepared by melt blending. Structure and some physical properties. J Appl Polym Sci 2002;86(6):1497–506.